

# A Novel Fusion Model for Battery Online State of Charge (SOC) Estimation

Yufang Li<sup>1,2,\*</sup>, Guofang Xu<sup>1</sup>, Bingqin Xu<sup>1</sup>, Yumei Zhang<sup>1</sup>

<sup>1</sup> Department of Vehicle Engineering, College of Energy & Power Engineering, Nanjing University of Aeronautics and Astronautics, Nanjing 210016, China

<sup>2</sup> Key Laboratory of Advanced Manufacture Technology for Automobile Parts (Chongqing University of Technology), Chongqing 400054, China

\*E-mail: [lyf2007@nuaa.edu.cn](mailto:lyf2007@nuaa.edu.cn)

Received: 2 October 2020 / Accepted: 16 November 2020 / Published: 30 November 2020

---

The state of charge (SOC) is a key parameter in battery management systems (BMSs). As an indirect parameter, accurately estimating the SOC has been an area of interest in battery research. To achieve online SOC estimation under variable temperature and discharge rate conditions, this paper proposes a novel modeling methodology for battery online SOC estimation based on an extended Kalman filter (EKF) and a backpropagation (BP) neural network and a method for calculating the true value of the battery SOC under these varying conditions for model validation. Three types of SOC estimation models are established and compared, involving an EKF model based on a second-order equivalent circuit model, a data-driven BP neural network model, and a fusion of the two models. Ultimately, the validity and rationality of the fusion modeling methodology for SOC online estimation proposed in this paper is verified by experimental data.

---

**Keywords:** SOC estimation, fusion modeling, EKF, BP, variable operating conditions

## 1. INTRODUCTION

The SOC reflects the current state of the remaining capacity of a battery, and its real-time acquisition is essential for the BMSs and energy management systems (EMSs) in electric vehicles. As an indirect parameter, accurate SOC estimation helps to prolong the service life of a battery, extend its cruising range and realize its safe control. There are many online estimation methods for assessing battery SOC, including the Coulomb counting method [1,2], methods based on the open circuit voltage (OCV) [3,4], the Kalman filter (KF) method [5-12], and methods based on neural networks [13-16]. The Coulomb counting method is typically used in actual engineering applications, but its disadvantage is that there can be error accumulations that lead to the SOC deviating from the actual value. Using the

OCV to estimate the SOC based on the OCV-SOC mapping relationship is not suitable for batteries with flat discharge platform characteristics; moreover, since it is difficult to obtain the online open circuit voltage, it is not suitable for online estimation. At present, Kalman filtering and its derivative algorithms are considered to be more effective methods for calculating a SOC, but they need a battery model to determine the functional relationship between the battery parameters such as current, voltage, internal resistance and SOC as the source of the state equation. Studies have shown that the proper selection of battery models is the key to ensuring the accuracy of these prediction algorithms [18].

However, the electrochemical working characteristics of batteries are complex, and many factors should be considered in the SOC calculation process, including battery charging/discharging rate, state of health (SOH), working temperature, and self-discharge factor. It is difficult to describe the nonlinear mapping relationship accurately between these multiple time-varying factors and the SOC in the complex and variable driving conditions inherent in electric vehicles. Therefore, the application of machine learning algorithms based on big data in SOC estimation has received more attention. However, a large amount of experimental data is needed for training and learning, resulting in considerable limitations in the real-time acquisition of SOCs. Researchers have begun to explore the fusion of model-driven estimation algorithms and data-driven estimation algorithms for SOC estimation [19-20]. Among them, the former are usually adopted to restrict the latter's SOC estimation results based on the electrochemical characteristics of the battery to reduce the latter's SOC calculation error.

To improve the prediction accuracy of SOC under time-varying conditions such as operating temperature and discharge rate, a new fusion modeling method of online battery SOC estimation based on an extended Kalman filter (EKF) and a backpropagation (BP) neural network is proposed. In addition, a method for calculating the true value of the battery SOC under these changing conditions is proposed for model verification. Finally, the effectiveness of the fusion modeling methodology is compared and verified.

## 2. RELATED WORKS

There has been great progress both at home and abroad in the use of Kalman filtering and its derivative algorithms to estimate the SOC of batteries. An SOC estimation method based on an improved EKF algorithm for electric vehicles under complex and variable operating conditions was proposed [9]. Higher SOC estimation accuracy was achieved by adopting an adaptive extended Kalman filter (AEKF) algorithm [10]. A dual AKEF was selected to estimate the parameters and states with consideration of the impact of the current discharge rate, and a least square support vector machine (LSSVM) was applied in the SOC prediction [11]. An unscented Kalman filter (UKF) algorithm was also studied to gauge the SOC according to a dynamic model to overcome linearization errors and control calculation problems of the EKF algorithm under strong nonlinear conditions [12].

At present, the topic of SOC online estimation using machine learning algorithms based on big data has been extensively explored, and it is still under study in terms of methodology and in specific applications. A three-layer feed-forward backpropagation (BP) artificial neural network was used to estimate and predict the SOC of a high-power Ni-MH rechargeable battery[14]. The Levenberg-

Marquardt (LM) algorithm was implemented in building a BP model of Li-ion phosphate batteries to obtain the battery SOC [15]. A novel method using a deep feed-forward neural network was adopted for battery SOC counting [16]. A data-driven method based on Gaussian process regression (GPR) was proposed, which provided a feasible solution for SOC estimation because of its superiority in accurately approximating nonlinear nonparametric modeling and probabilistic prediction capabilities [17].

The premise of a model-driven SOC estimation algorithm is a suitable model with moderate complexity to describe the electrochemical characteristics of a battery, which can improve the prediction accuracy to some extent. Equivalent circuit models are widely used in SOC estimation, including first-order equivalent circuit models, PNGV models, second-order RC equivalent circuit models, fractional-order models, and high-order equivalent circuit models. To attain a more accurate battery model with moderate complexity, seven existing representative electrochemical models or equivalent circuit models were identified by online parameter identification methods [21]. A reduced-order model was proposed to characterize the dynamic voltage response of Li-ion batteries. Assuming that the active material was uniform, the ion concentration and potential in the liquid phase were predicted, and the voltage response characteristics under large currents were established [22]. The influence of temperature on charge transfer resistance, diffusion resistance and electrolyte resistance was analyzed, and the results showed that regardless of the frequency range, the correlation between resistance and SOC was weak [24]. An enhanced first-order RC circuit model was used to characterize the battery state at different temperatures with a simple structure, but the accuracy was not high [25]. A novel fractional order model of a battery was proposed in which both the Butler-Volmer equation and the fractional calculus of constant phase element were considered, and an SOC identification method combining least squares and nonlinear optimization algorithms was discussed [26].

As mentioned above, exploring new methods to improve the accuracy of battery SOC estimation under complex and changeable driving conditions is still an area of research interest both at home and abroad. In view of these efforts, this paper proposes a fusion modeling method for online SOC calculation based on a second-order battery equivalent circuit model, a BP neural network and an EKF algorithm. The research flow chart is shown in Figure 1. The chapter structure of this paper is as follows. Section 0 presents a battery equivalent circuit model and parameter identification. In Section 0, the principle of the battery SOC estimation algorithm is introduced, including improved EKF-based SOC estimation, BP-based SOC estimation and fusion modeling. The acquisition of data required for battery SOC estimation and the results and analysis of battery SOC estimation are provided in Section 0. Finally, Section **Error! Reference source not found.** further discusses and concludes this paper.

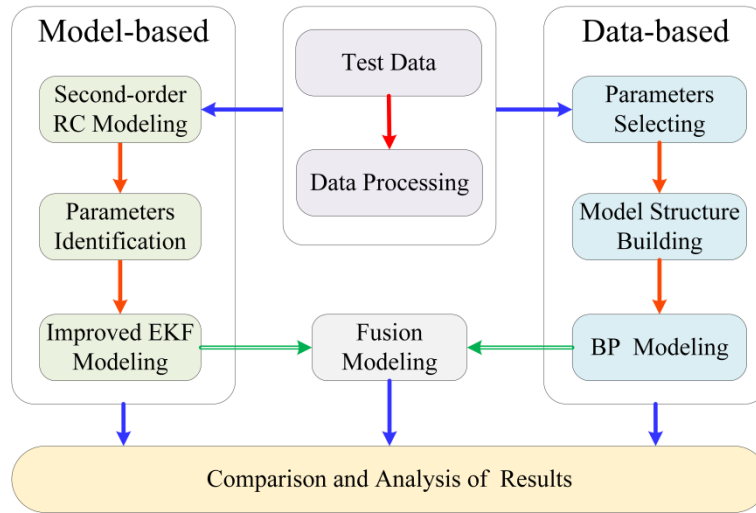


Figure 1. Research flow chart

### 3. MODELING AND PARAMETER IDENTIFICATION

#### 3.1. Second-order RC Equivalent Circuit Model

A second-order RC equivalent circuit model is adopted in this paper due to its high accuracy in characterizing the electrochemical characteristics of a battery with low complexity [9]. This model includes an ideal voltage source  $U_{oc}$ , the ohmic internal resistance of the battery  $R_0$ , and two RC circuits in parallel [27], as shown in Figure 2.

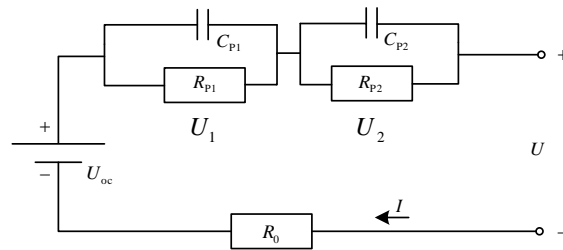


Figure 2. Second-order RC equivalent circuit model

The equation of state is:

$$\begin{bmatrix} U_1(k) \\ U_2(k) \\ SOC(k) \end{bmatrix} = \begin{bmatrix} e^{-\frac{T_s}{R_{p1}C_{p1}}} & 0 & 0 \\ 0 & e^{-\frac{T_s}{R_{p2}C_{p2}}} & 0 \\ 0 & 0 & 1 \end{bmatrix} \begin{bmatrix} U_1(k-1) \\ U_2(k-1) \\ SOC(k-1) \end{bmatrix} + \begin{bmatrix} R_{p1} \cdot (1 - e^{-\frac{T_s}{R_{p1}C_{p1}}}) \\ R_{p2} \cdot (1 - e^{-\frac{T_s}{R_{p2}C_{p2}}}) \\ \frac{\eta_k T_s}{C_N} \end{bmatrix} I(k-1) + \omega(k-1) \quad (1)$$

The observation equation is:

$$U(k) = U_{oc} - U_1(k) - U_2(k) - I(k)R_0 + v(k) \quad (2)$$

where  $R_{P1}$  and  $R_{P2}$  are the battery polarization resistances,  $C_{P1}$  and  $C_{P2}$  are the battery polarization capacitors,  $R_0$  is the battery ohmic resistance,  $U_1$  and  $U_2$  are the voltages across  $R_{P1}$  and  $R_{P2}$ , respectively,  $\eta_k$  is the charge and discharge efficiency,  $C_N$  is the actual total capacity of the battery in the current state,  $U_{oc}$  is the open battery voltage,  $I$  is the battery current, and the sign indicates that the charging is positive and the discharging is negative.  $U$  is the battery terminal voltage. In addition,  $\omega(k-1)$  represents Gaussian white noise with a mean of 0 and a variance of  $Q$ , and  $v(k)$  represents Gaussian white noise with a mean of 0 and a variance of  $R$ .

### 3.2. Parameter Identification

Relevant parameters of the equivalent circuit model, such as open circuit voltage and ohmic internal resistance, are effectively identified to describe the electrochemical characteristics of the specific battery [28]. With respect to parameter identification methods, much work has been reported recently in these fields, involving genetic algorithms, particle swarm optimization algorithm experimental methods [29], least squares methods[30], hybrid pulse power characteristic (HPPC) tests [31] and so on. In this paper, the HPPC test method is used to identify the model parameters of the battery at different temperatures and different discharge rates.

#### 3.2.1. Identification of Open Circuit Voltage

The operating temperature has a large effect on the open circuit voltage, while the discharge rate has a smaller impact [32]. Therefore, the HPPC test is carried out at ambient temperatures of 0°C, 5°C, 10°C, 15°C, 20°C and 25°C, with a discharge rate of 0.3C. Each test consists of 11 pulses at each discharge condition, with the SOC varying from 100% to 0% with an interval of 10% SOC. The current and voltage curves of HPPC tests at different temperatures are shown in Figure 3(a), which are used to obtain the steady-state open circuit terminal voltage of the battery under different SOC. The OCV-SOC curves of the battery at different temperatures are obtained by polynomial fitting, as shown in Figure 3(b).

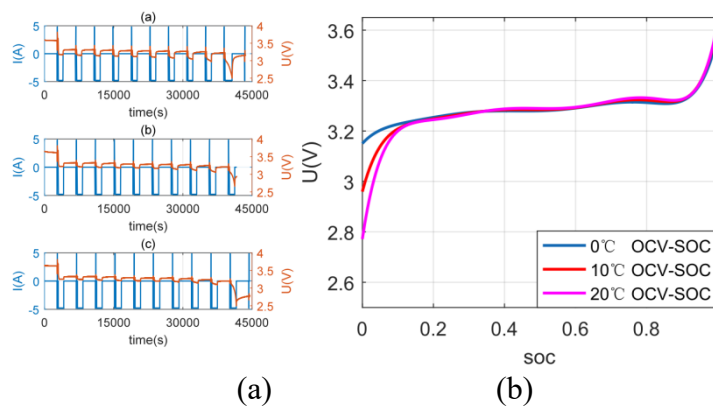


**Figure 3.** HPPC test and results: (a) current and voltage curves; (b) OCV-SOC curves

### 3.2.2. Resistance and Capacitance Identification

The HPPC test is carried out at 0°C, 5°C, 10°C, 15°C, 20°C and 25°C, and the discharge rates are 0.3C, 0.5C, 1.0C, 1.5C and 2.0C, respectively, to identify ohmic resistance  $R_0$ , battery polarization resistances  $R_{p1}$  and  $R_{p2}$ , and battery polarization capacitors  $C_{p1}$  and  $C_{p2}$  to finally create a table of battery parameters with regard to temperatures and discharge rates. The extracted single HPPC test current-voltage curve and battery zero input response fitting curve are shown in Figure 4. Figure 4(b) shows a section of voltage from  $U_2'$  to  $U_3$  for curve fitting. The equations for the model parameters and battery voltage can be obtained by the curve. Then, the above parameters are calculated under different temperature and SOC conditions based on formula (3).

$$U = U_{oc} - IR_0 - IR_{p1}(1 - e^{-t/\tau_1}) - IR_{p2}(1 - e^{-t/\tau_2}) \quad (3)$$

where  $C_{p1} = \tau_1 / R_{p1}$  and  $C_{p2} = \tau_2 / R_{p2}$ .

The other part of the experimental data was used to verify the accuracy of the model identification results, as shown in Figure 5. It can be proven that the model identification result has good accuracy, as illustrated by the maximum difference of 30 mV between the model output and the measured value of the battery terminal voltage.

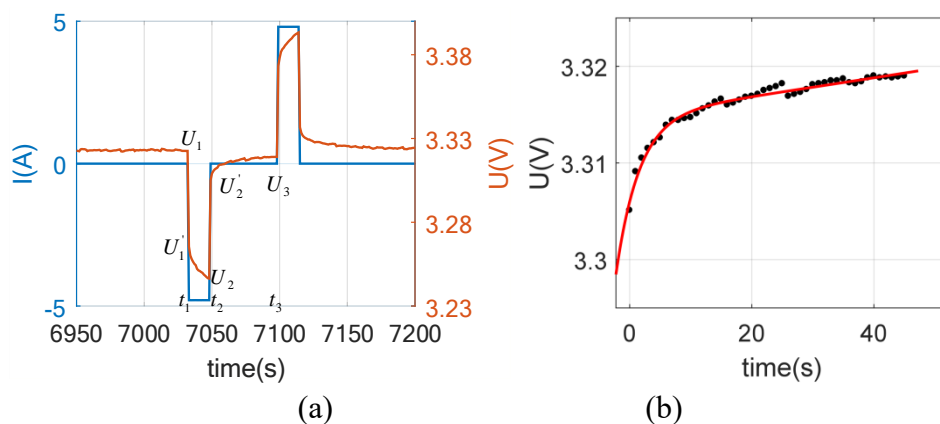


**Figure 4.** Parameter identification based on HPPC: (a) current-voltage curve of the single-time HPPC test; (b) battery zero-input response fitting curve.

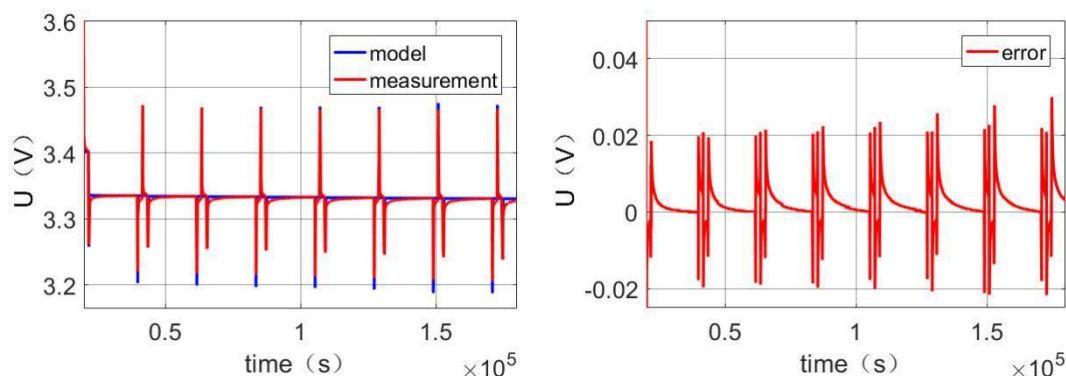


**Figure 5.** Model and measurement results of battery terminal voltage

## 4. SOC ESTIMATION PRINCIPLE

### 4.1. Improved EKF-based SOC Estimation

SOC estimation is currently performed with EKF and its derivative algorithms because of its superiority in the multidimensional stochastic estimation of state variables for nonlinear systems [33]. Generally, in an SOC estimation algorithm based on EKF, the total capacity of the battery does not change or is a function of a single variable such as temperature or discharge rate. Actually, because the SOC reflects the remaining proportion of the available power in the current battery SOH, the maximum actual total capacity required for SOC calculation needs to vary with temperature and discharge rate [34]. Therefore, this article obtains the actual total capacity of the battery, which reflects the influence of battery SOH on SOC prediction through experiments at different temperatures and discharge rates to improve the EKF-based SOC estimation. By averaging the three tests under the same conditions, the amount of power released by the battery is calculated, and the mapping relationship is established by interpolation. Based on a second-order RC equivalent circuit model, the EKF algorithm is improved through the above correction calculation of the actual total capacity.

The recursive formulas are as follows.

Filter initial value is:

$$x_{0/0} = E(x_0), P_{0/0} = \text{var}(x_0) \quad (4)$$

The state estimate is:

$$x_{k/k-1} = A_{k-1}x_{k-1/k-1} + B_{k-1}I_k \quad (5)$$

The error covariance estimation matrix is:

$$P_{k/k-1} = A_{k-1}P_{k-1/k-1}A_{k-1}^T + \Gamma_{k-1}Q_{k-1}\Gamma_{k-1}^T \quad (6)$$

The Kalman gain matrix is:

$$K_k = P_{k/k-1}C_k^T (C_k P_{k/k-1} C_k^T + R_k)^{-1} \quad (7)$$

The observed value is:

$$U_k = U_{oc,k} - U_{1,k} - U_{2,k} - R_{0,k}I_k \quad (8)$$

The state filter value is:

$$x_{k/k} = x_{k/k-1} + K_k (y_k - C_k x_{k/k-1}) \quad (9)$$

The filtering error covariance matrix is:

$$P_{k/k} = (E - K_k C_k) P_{k/k-1} \quad (10)$$

where  $x_{k/k-1}$  is the predicted value of the estimated state.  $x_{k/k}$  is the filtered value of the estimated state.  $P_{k/k}$  is the filter error covariance matrix.  $P_{k/k-1}$  is the prediction error covariance matrix.  $Q_k$  is the process excitation noise covariance matrix.  $\Gamma_k$ ,  $K_k$ ,  $y_k$  and  $E$  are the interference matrix, Kalman gain matrix, observation value, and identity matrix, respectively.

#### 4.2. BP-based SOC estimation

A BP (backpropagation) neural network is one of the most widely used neural network models that can learn and store many input-output model mappings without prior descriptions of the mathematical equations of the mapping relationship. Its learning rule uses the gradient descent method by backpropagation to constantly adjust the network weights and thresholds and minimize the error sum of squares in the network. A BP neural network model of topological structures includes an input layer, hidden layer, and output layer, as shown in Figure 6. [14]. It has been proven that when the number of hidden layer neurons is sufficient, a three-layer forward network can map the nonlinear function with arbitrary precision [35]. Therefore, in this paper, a BP neural network is used for the SOC estimation of Li-ion batteries. The working voltage  $U$ , working current  $I$ , ambient temperature  $T$ , and actual total capacity  $Q$  are the inputs for the BP model.

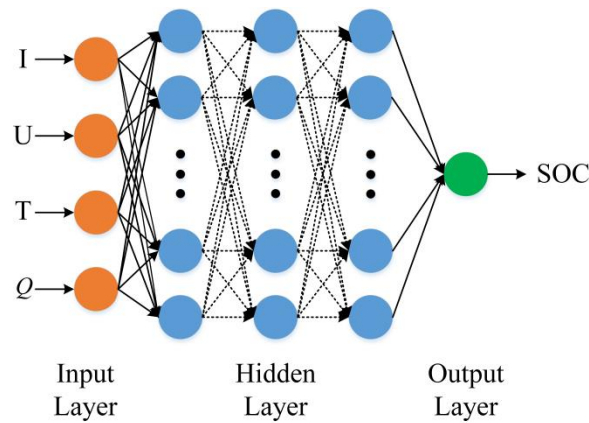


**Figure 6.** BP neural network structure diagram

First, a three-layer BP neural network model is established with an input vector  $[U, I, T, Q]$ , where  $Q = f(I, T, SOH)$ , the number of input nodes  $n=4$ , and the output vector  $[SOC]$  and the number of output nodes  $l=1$ . In addition, the tansig activation function and the mean square error performance function are determined.

Second, the SOC calculation result of the BP model is taken as the observation value of the EKF algorithm for filtering purposes and for improving the accuracy of SOC estimation. The state-space equation are as follows.

Equation of state:

$$SOC(k+1) = SOC(k) - \eta \frac{I \cdot \Delta t}{C_N} \quad (11)$$

Observation equation:

$$SOC_{BP}(k+1) = SOC(k) \quad (12)$$

where  $C_N$  is the actual total capacity of the battery in the current state determined by the above experimental data and  $SOC_{BP}(k+1)$  is the estimation result of the BP neural network.

### 4.3. Fusion modeling

A novel fusion modeling methodology for SOC prediction is proposed in this paper by combining the improved EKF algorithm and the BP neural network. The mechanism is as follows: the improved EKF estimation and BP neural network estimation are calculated, and the difference ( $SOC_{EKF} - SOC_{BP}$ ) is simultaneously filtered by EKF. The filtered state equation and observation equation are as follows:

$$\begin{cases} X_k = AX_{k-1} + \omega_{k-1} \\ Y_k = CX_k + \nu_{k-1} \end{cases} \quad (13)$$

where  $Y = [SOC_{EKF} - SOC_{BP}]^T$ ,  $A = diag(1)$ ,  $C = diag(1)$ , and  $\omega$ ,  $\nu$  are Gaussian noise. The filtered result minus the improved EKF result is regarded as the output of the fusion model, namely,  $SOC = SOC_{EKF} - X$ .

Fusion modeling combines the model-driven EKF algorithm with the data-driven neural network algorithm. The former model, based on the equivalent circuit, has characteristics that can accurately describe the working state of the battery. Its model is relatively simple, but the accuracy of the calculation results is not very high. The latter requires big data to obtain accurate results, is characterized by more complexity and is not suitable for complex working conditions with state changes. The fusion modeling is based on the advantages of these two algorithms and uses the more accurate results of the neural network algorithm to modify the estimated value of the EKF algorithm to make the SOC estimation result more accurate. In addition, the fusion method is used to avoid result errors caused by data problems.

## 5. ALGORITHM VERIFICATION AND ANALYSIS

### 5.1. Data Acquisition

A Chroma17020 battery pack test system and a TERCHY programmable environment tester are used for the battery test, as shown in Figure 7. The latter provides a temperature environment of  $-50^\circ\text{C} \sim 80^\circ\text{C}$ , which meets the requirements of temperature variation. The chroma sampling frequency is set to 1 Hz to simulate the actual operation of BMS. The test battery is a prismatic Li-ion phosphate power battery with a rated capacity of 16 Ah, a charging cutoff voltage of 3.65 V and a discharging cutoff voltage of 2.5 V.

The battery SOC estimation algorithms proposed in this paper are verified under constant and variable operating conditions of temperatures and discharge rates. The constant working conditions include discharging a full-charge battery at discharge rates of 0.3C, 0.5C, 1C, 1.5C, and 2C under temperatures of  $0^\circ\text{C}$ ,  $5^\circ\text{C}$ ,  $10^\circ\text{C}$ ,  $15^\circ\text{C}$ ,  $20^\circ\text{C}$  and  $25^\circ\text{C}$ , respectively, and discharging to the cutoff

discharge voltage. The variable working conditions include the discharge rate during battery discharge increasing from 0.3C to 2C, then decreasing from 2C to 0.3C, and the temperature increasing from 10°C to 20°C, then decreasing from 20°C to 0°C, and finally returning to 10°C.

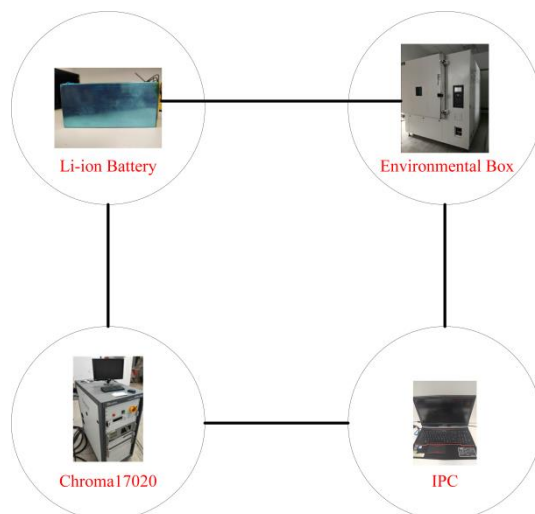


Figure 7. Test equipment setup diagram

## 5.2. Result Analysis

### 5.2.1. Constant Temperature and Discharge Rate

The SOC estimation results are shown in **Table 5.1**. Under all conditions of constant temperature and discharge rate, the SOC estimation result of the fusion model is the most accurate, followed by BP, and the improved EKF is the worst result as illustrated by the largest error range fluctuation, especially at 10°C and 20°C; its accuracy is obviously lower than that of the BP algorithm. Compared with the improved EKF and BP, the fusion model based on the above two algorithms achieves the best result.

Table 5.1. The results of constant temperature and discharge rate

	0°C		10°C		20°C	
	ERROR	RMSE	ERROR	RMSE	ERROR	RMSE
EKF	1.23%	0.7704%	2.38%	0.6598%	1.88%	1.5509%
BP	1.11%	0.6216%	1.16%	0.5849%	0.91%	0.7727%
Fusion Model	1.00%	0.5991%	0.86%	0.4214%	0.80%	0.4893%

Other scholars and researchers have also conducted a lot of research on the combination of neural

network model and EKF to estimate battery SOC. Some literatures use the method of segmented research on the SOC interval of the battery, and the SOC error is about 3%[19,20]. Compared with those models, the method adopted in this paper has the applicability of the whole SOC range and the accuracy is higher.

More details of the results are shown in Figure 8. It can be seen in the figure that the convergence of the fusion model is better than that of EKF and BP. For the same initial value deviation, the fusion model converges to the true value of the SOC faster. At 10°C, the EKF estimate result has a larger error than the other two temperatures, but the fusion model has a smaller error. It can be seen that the estimation stability of the fusion model is better, which can reduce the accidental errors caused by the model.

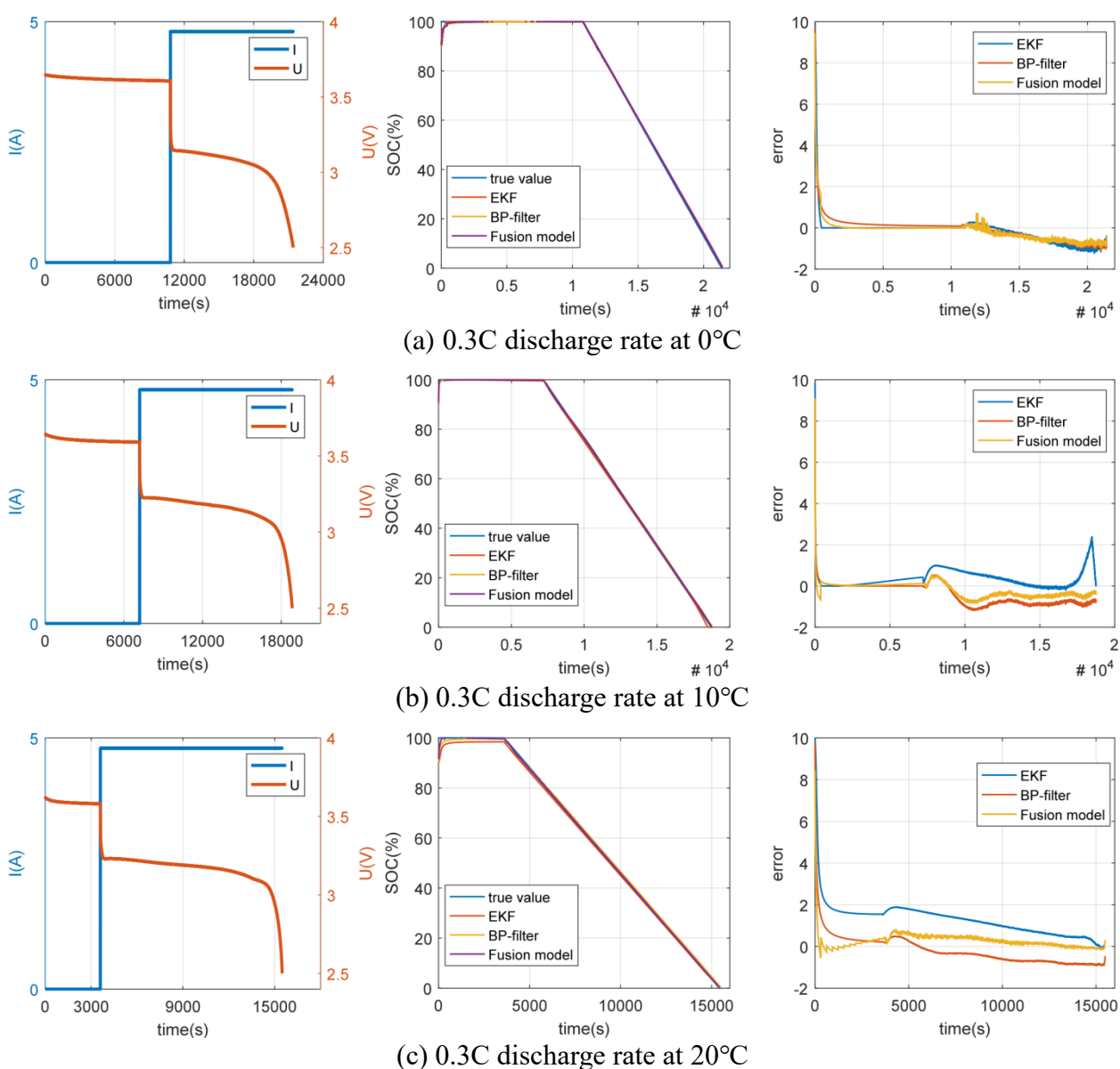


Figure 8. Results of constant temperature and discharge rate

5.2.2 Variable Temperatures and Discharge Rates

The calculation of battery SOC under varying temperature and discharge rate conditions is different from that under constant conditions. In this paper, a method for calculating the true value of SOC under the varying conditions is presented. The battery discharges completely from a fully charged state. Its discharge process is divided into several sections with the same discharge rate, and only the temperature changes in each section. Therefore, the actual battery capacity is only related to the temperature. The total SOC change value  $SOC_1, SOC_2 \dots SOC_i$  of each segmented discharge process is calculated based on the interpolation. In the last segmented discharge process, the battery SOC changes from  $SOC_i^e + SOC_i$  to 0%. In addition, in the previous segmented discharge process, when the battery is cut off, the SOC is  $SOC_{i-1}^e = SOC_i^e + (I_i \cdot t_i) / C_{N_{i-1}}^e$ , of which  $SOC_{i-1}^e$  is the discharge cutoff SOC of the battery in the previous segmented discharge process.  $SOC_i^e$  is the discharge cutoff SOC of the battery in the current segmented discharge process.  $I_i$  is the current of the battery in the current process.  $t_i$  is the battery discharge time in the current process.  $C_{N_{i-1}}^e$  is the current actual total capacity of the battery when it is discharged in the previous segment discharge process.

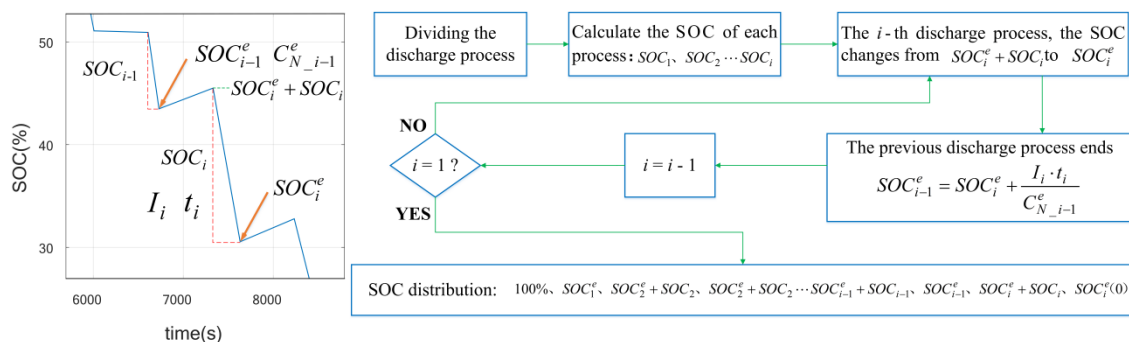


Figure 9. Flow chart of the calculation method of the battery SOC true value

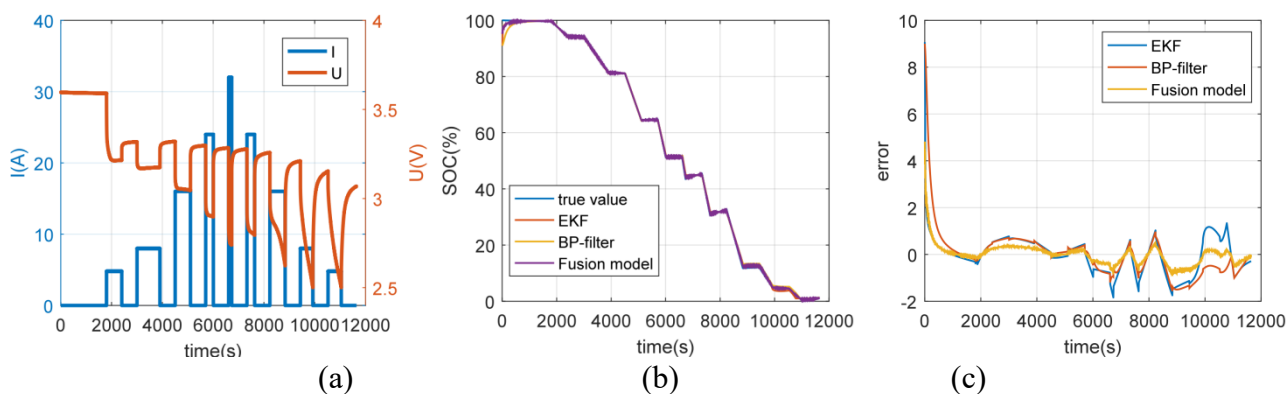


Figure 10. Results of variable temperature and discharge rate: (a) current voltage curve; (b) SOC estimation result; (c) error.

By analogy, the starting SOC value and the ending SOC value of the battery in each segmented discharge process can be obtained. The SOC value is divided into the entire discharge process according to the time distribution, and the battery SOC value during the entire discharge process can be obtained, that is, the battery SOC true value distribution, namely,  $100\%$ ,  $SOC_1^e$ ,  $SOC_2^e + SOC_2$ ,  $SOC_2^e \cdots SOC_{i-1}^e + SOC_{i-1}$ ,  $SOC_{i-1}^e$ ,  $SOC_i^e + SOC_i$ , and  $SOC_i^{(0)} \cdot SOC_i^e$  is the battery SOC at the end of the  $i$ -th stage. The method flowchart is shown in Figure 9.

The actual SOC values in each state calculated by reverse iteration above are used to evaluate and compare the performance of each online SOC estimation algorithm. The estimated results are shown in Figure 10. For the entire discharge process, the RMSE of the improved EKF is 1.0744%, the RMSE of BP is 0.7740%, and the RMSE of the BEFM is 0.4315%. The maximum error of the improved EKF is 1.84%, the maximum error of BP is 1.57%, and the maximum error of the fusion model is 0.91%. Under the conditions of variable temperature and discharge rate, the BP algorithm is more accurate in estimating the battery SOC than the improved EKF algorithm. Both algorithms are unstable in battery SOC estimation under variable conditions. This is due to the influence of the temperature and discharge rate on the actual total capacity of the battery at the current temperature discharge rate and the rise in battery capacity caused by internal electrochemical effects when the battery is left standing. Compared with the improved EKF and BP, the results of the fusion model for battery SOC are smoother and more accurate. Because the calculated battery SOC value changes due to operating conditions and standing, the SOC before and after standing will change, so there will be a zigzag shape in the error curve.

## 6. CONCLUSIONS

In this paper, an online estimation method for battery SOC that combines an improved EKF and BP model is proposed, and the principles and results of the SOC estimation based on the improved EKF, the BP network and the fusion of the improved EKF and BP are compared and analyzed. In the process of SOC estimation, the actual total capacity of the battery under the conditions of variable temperature and discharge rate is adopted to improve the accuracy of SOC online estimation during discharge under variable conditions. At the same time, to objectively evaluate the accuracy of the SOC online estimation method, this paper also proposes a method of reverse-calculating the true value of battery SOC at each moment by using offline data, which can be used for the correction of the SOC online estimation method.

The results show that the proposed SOC online estimation fusion model has high accuracy and good robustness under the operating conditions of both constant and variable temperatures and discharge rates, which indicates the rationality of the fusion modeling methodology for SOC estimation based on a model-based EKF and a data-based BP algorithm. In addition, it should be noted that the operating conditions of the battery with variable temperatures and discharge rates tested in the experiment in this paper are limited, which may not fully reflect more complex operating conditions. In future research, we will further enrich and refine the test operating condition data.

## References

1. K. S. Ng, C. S. Moo, Y. P. Chen and Y. C. Hsieh, *Appl. Energy*, 86.9(2009)1506.
2. A. Purwadi, A. Rizqiawan, A. Kevin and N. Heryana, State of charge estimation method for lithium

- battery using combination of coulomb counting and adaptive system with considering the effect of temperature. *The 2nd IEEE Conference on Power Engineering and Renewable Energy, Bali, Indonesia*, 2015, 91-95.
3. Y. Deng, Y. Hu and Y. Cao, *Intelligent Computing in Smart Grid and Electrical Vehicles*, 463(2014)258.
  4. S Lee, J. Kim, J. Lee and B. H. Cho, *J. Power Sources*, 185.2(2008)1367.
  5. G. L. Plett, *J. Power Sources*, 134.2(2004)262.
  6. C. Hu, B. D. Youn and J. Chung, *Appl. Energy*, 92(2012)694.
  7. J. Lee, O. Nam and B. H. Cho, *J. Power Sources*, 174.1(2007)9.
  8. W. He, N. Williard, C. Chen and M. Pecht, *Microelectron. Reliab.*, 53.6(2013)840.
  9. D. Xu, X. Huo, X. Bao, C. Yang, H. Chen and B. Cao, Improved EKF for SOC of the storage battery, *IEEE International Conference on Mechatronics and Automation, Takamatsu, Japan*, 2013, 1497-1501.
  10. Y. Guo, Z. Zhao and L. Huang, *Energy Procedia*, 105(2017)4146.
  11. Z. Deng, L. Yang, Y. Cai, H. Deng and L. Sun, *Energy*, 112(oct.1)(2016)469.
  12. X. Zhang, J. Wu and G. Kang, SOC estimation of Lithium battery by UKF algorithm based on dynamic parameter model, *International Conference on Ubiquitous Robots & Ambient Intelligence, Xi'an, China*, 2016, 945-950.
  13. L. W Kang, X. Zhao and J. Ma, *Appl. Energy*, 121(2014)20.
  14. C. Cai, D. Du, Z. Liu and J. Ge, State-of-charge (SOC) estimation of high power Ni-MH rechargeable battery with artificial neural network, *Proceedings of the 9th International Conference on Neural Information Processing, Singapore, Singapore*, 2002, 2, 824-828.
  15. A. Yin, W. Zhang, H. Zhao and H. Jiang, *J. Electronic Measurement & Instrument*, 25.5(2011)433.
  16. C. Ephrem, P. J. Kollmeyer, P. Matthias and E. Ali, *J. Power Sources*, 400(2018)242.
  17. D. Zeng, X. Hu, X. Lin, Y. Che and W. Guo, *Energy*, (2020)118000.
  18. G. L. Plett, *J. Automotive Safety and Energy*, 10.03(2019)249.
  19. M. Charkhgard and M. Farrokhi, State-of-charge estimation for Li-ion batteries using neural networks and EKF, *IEEE Transactions on Industrial Electronics*, 2010, 57(12), 4178-4187.
  20. W. He, N. Williard, C. Chen and M. Pecht, *Int. J. Electr. Power Energy Syst.*, 62(2014)783.
  21. H. He, R. Xiong, H. Guo and S. Li, *Energy Conversion & Management*, 64(2012)113.
  22. J. Marcicki, M. Canova, A. T. Conlisk and G. Rizzoni, *J. Power Sources*, 237.3(2013)310.
  23. J. Li, L. Wang, C. Lyu and M. Pecht, *Energy*, 133(2017)572.
  24. S. Skoog and S. David, *J. Energy Storage*, 14(2017)39.
  25. Y. Xing and K. L. Tsui, *Proceedings of the Institute of Industrial Engineers Asian Conference, Springer Singapore*, (2013)Singapore, Singapore.
  26. R. Xiong, J. P. Tian, F. C. Sun and W. X. Shen, A novel fractional order model for state of charge estimation in lithium ion batteries, *IEEE Transactions on Vehicular Technology*, 2019, 69, 4130-4139.
  27. Z. Cheng, Q. Y. Zhang and Y. H. Zhang, *Advanced Materials Research*, 805-806(2013)1659.
  28. H. Liu, Study on SOC estimation method of Li-ion battery based on EKF for electric vehicles, Master, Beijing Jiaotong University, Beijing, China, 2010.
  29. V. Sangwan, A. Sharma, R. Kumar and A. K. Rathore. Equivalent circuit model parameters estimation of Li-ion battery: C-rate, SOC and Temperature effects, *IEEE International Conference on Power Electronics, Trivandrum, India*, 2016, 1-6.
  30. V. H. Duong, H. A. Bastawrous, K. C. Lim, K. W. See, P. Zhang and S. X. Dou. SOC estimation for LiFePO<sub>4</sub> battery in EVs using recursive least-squares with multiple adaptive forgetting factors. *The 3rd International Conference on Connected Vehicles & Expo (ICCVE), Vienna, Austria*, 2014, 520-521.
  31. B. X. Sun, J. C. Jiang and Z. G. Wang, *Advanced Materials Research*, 403-408(2011)4398.
  32. W. Xu, J. L. Xu, B. L. Liu, J. J. Liu and X. F. Yan, *Energy Science and Engineering*, 8 (2020) 12
  33. Risfendra, Y. S. Kung and L. C. Huang, Design and digital hardware implementation of a sensorless controller for PMSM drives using LF signal injection and EKF, *International Conference on Applied System Innovation (ICASI), Sapporo, Japan*, 2017, 1281-1284.

34. Y. He, X. T. Liu, C. B. Zhang and Z. H. Chen, *Appl. Energy*, 101(2013)808.
35. W. Jian, X. Jiang, J. Zhang, Z. Xiang and Y. Jian. Comparison of SOC Estimation Performance with Different Training Functions Using Neural Network, *Uksim International Conference on Modelling & Simulation, Cambridge, UK, 2012*, 459–463.

© 2021 The Authors. Published by ESG ([www.electrochemsci.org](http://www.electrochemsci.org)). This article is an open access article distributed under the terms and conditions of the Creative Commons Attribution license (<http://creativecommons.org/licenses/by/4.0/>).